Paste 2023 – GW Wilson, NA Beier, DC Sego, AB Fourie & D Reid (eds)

doi:10.36487/ACG_repo/2355_67

Experimental validation of a prediction model of the compressive strength of cemented rockfills

G Rafraf *Université du Québec en Abitibi-Témiscamingue, Canada*

T Belem *Université du Québec en Abitibi-Témiscamingue, Canada*

H Mrad *Université du Québec en Abitibi-Témiscamingue, Canada*

L-P Gélinas *Agnico Eagle Mines Limited, Canada*

A Krichen *National School of Engineering of Sfax, Tunisia*

Abstract

Underground mine backfilling promotes solid waste to be returned as cementitious material either in the form of cemented paste backfill – CPB – (using tailings) or in the form of cemented rock fill – CRF – (using crushed waste rock, WR). The cement or binder addition is intended to develop a required unconfined compressive strength (UCS) value to ensure ground stability during mining operations. While CPB is the most common type of mine backfill used in underground mining operations, CRF is only used when high compressive strength is required to increase productivity. Despite the performance of CRF, this type of backfill is not much studied or optimised. The main objective of this study is to validate experimentally a newly developed semi-empirical model for predicting the UCS of CRF. This model considers various physical parameters of CRF materials such as the types of binder (e.g. general use Portland cement –GU, GU-fly ash, GU-ground granulated blast furnace slag, etc.) and their mass proportion (binder rate B_w), the water-to-cement ratio (W/C), the type of WR (according to its relative density D_R) and the grain size distribution, and the curing time (t). To this end, numerous cylindrical CRF specimens are prepared by varying the W/C, the type of binder, the binder rate B_w (4–8%), the type of WR and the average diameter (d) of the particles. Preliminary results show that the accuracy of the predicted UCS values of various laboratory-prepared CRF mix recipes is satisfactory with a high coefficient of correlation ($R \geq 0.9$). Therefore, it is reasonable to adopt the proposed CRF strength prediction model for laboratory-prepared specimens that can be scaled up in situ by developing an efficient CRF preparation quality control (QC) procedure.

Keywords: *unconfined compressive strength, cemented rockfill, semi-empirical prediction model, experimental validation, quality control*

1 Introduction

Using backfills in mining operations is one of the most appreciated methods to better manage tailings and waste rock (WR) generated after extraction and processing of the ore. Cemented mine backfills have three major components: the granular skeleton (e.g. fine tailings, crushed WR or borrow aggregate), the binding agent (e.g. general use Portland cement – GU – or mineral additions such as supplementary cementitious materials, namely fly ash, slag etc.) and the mixing water (Belem & Benzaazoua 2008). With technological advances, underground mines are becoming increasingly deeper (e.g. ≥ 3.2 km at the LaRonde mine in Abitibi-Témiscamingue region, Quebec, Canada) and the natural in situ stresses generated during ore extraction are very high. These stresses can cause local seismic occurrences that lead to rock vibration with disastrous consequences for the mine. In such hostile and damaging conditions that constitute the underground environment, the use of cemented rock fills (CRF) can provide a safe and reliable solution to reduce these hazards. Moreover, the required unconfined compressive strength (UCS) of a backfill to resist failure during deep mining operations can exceed 4 MPa (Villaescusa 2003; Hane et al. 2017a, b). For this reason and due to its high compressive strength (in the range 3–17 MPa), it will be appropriate to opt for CRF

in deep mining operations. Despite the performance of CRF, this type of backfill is understudied and under-optimised (Gonano et al. 1978; Yu 1989; Stone 1993; Hedley 1995; Farsangi et al. 1996; Farsangi 1996; Annor 1999; Hane et al. 2018).

Among these authors, some have proposed semi-empirical models for predicting the UCS of CRFs based mainly on the mass ratio of the binder (B), and the final porosity (n) of the mixture (Mitchell & Wong 1982; Arioglu 1984; Yu 1989; Lamos & Clark 1993; Hedley 1995; Annor 1999). Yet none of these previous empirical models take into account all of the physical parameters of CRF, such as the types of binder (e.g. GU, and blended binders such as GU-fly ash, GU-ground granulated blast furnace slag etc.), the water-to-cement ratio (W/C), the type of the WR (according to its specific gravity – G_s/relative density – D_R), the grain size distribution and the curing time (t).

2 Background

2.1 Semi-empirical predictive model of the CRF compressive strength

To compensate for the lack of an analytical model, Belem (2020) developed a new semi-empirical model for predicting the UCS of CRFs by relying on existing limited laboratory data (Hane et al. 2018). This new model considers several physicochemical parameters (input variables) of the CRF mixtures, such as the types of binder, the B_w, (W/C), the lithology of the WR (G_s or D_R), the grain gradation (particle diameters d_{min} and d_{max}) and curing time.

The new semi-empirical model for predicting the compressive strength (UCS_{pred}) of CRFs is given as follows (Belem 2020):

$$UCS_{pred} = A_c \times G_{s-WR}\left(r_d = \frac{D_{50}}{d_{\min}}\right)^{-n}\left(\left[1+t_r\right]^{-1.625}\left[1+\left(\frac{W}{C}\right)^{-2}+\left(B_{w\%}\right)^{1.5}\right]^{-2}\right)^{-m} \quad (1)$$

where:

- A_c = the 'critical' UCS of the intact rock composing the WR (kPa).
- $G_{s\text{-}WR}$ = specific gravity or relative density of the WR.
- r_d = [D_{50}(mm)/d_{min}(mm)] = particle size ratio between the median size (D_{50} = the diameter corresponding to 50% passing of the WR particles) and the smallest particle size (d_{min} is fixed at 10 mm = fine particles).
- t_r = relative curing time = (t/10 days) = curing time t (day)/10 days.
- W/C = W/C ratio, $B_{w\%}$ = binder rate = $100 \times M_{binder}/M_{waste\text{-}rock}$.
- n and m = particle size adjustment factor and exponent expressing the effect of the binder type respectively, and which are determined empirically.

The value of n has been determined empirically to be 0.35. As for the values of m, they depend on the type of binding agent used in the mixture (GU, ground granulated blast furnace slag, and fly ash – or FA).

Table 1 Empirical values of the constant A_c and the exponent m for different types of binding agents

Types of binder	Constant A_c (kPa)	Exponent m
10GU/90Slag	101.680	0.3822
50GU/50FA	23.551	0.5653
Undefined	50.959	0.4692

By rearranging Equation 1, it is possible to isolate in turn the key parameters controlling the strength development in view of the CRF mix recipes' formulations or the implementation of a procedure for the quality control (QC) of CRF, namely the $B_{w\%}$ in percent, and the W/C or water-to-binder ratio (W/C) which are given by the following relationships:

$$\frac{W}{C}=\left(\sqrt{\left(1+t_r\right)^{-1.625}\left(\frac{UCS_{\text{target}}}{A_c\cdot\left[r_d\right]^{-n}}\right)^{\frac{1}{m}}-\left(B_{w\%}\right)^{1.5}-1}\right)^{-\frac{1}{2}} \tag{2}$$

$$B_{w\%}=\left(\sqrt{\left(1+t_r\right)^{-1.625}\left(\frac{UCS_{\text{target}}}{A_c\cdot\left[r_d\right]^{-n}}\right)^{\frac{1}{m}}-\left(\frac{W}{C}\right)^{-2}-1}\right)^{\frac{2}{3}} \tag{3}$$

In Equations 2 and 3, UCS_{pred} has been replaced by the target of the UCS (UCS_{target}) for either CRF mix recipes' formulations or for the QC of CRF. In addition to these two physicochemical parameters, two other physical parameters are important to know: the wet or total density (ρ_h or ρ_{wet}) and the total porosity (*n*), which are given by the following relations:

$$\rho_h=\left(\frac{G_{s-CRF}}{\rho_{s-CRF}}+\frac{1}{\rho_{s-CRF}}\left[\frac{\left(1-G_{s-CRF}\right)\left(1+\frac{1}{B_w}\right)}{1+\frac{1}{B_w}+\frac{1}{S_r}\left(\frac{W}{C}\right)}\right]\right)^{-1}=\rho_{wet} \tag{4}$$

$$n=1-\frac{1+\frac{1}{B_w}}{G_{s-CRF}\left(1+\frac{1}{B_w}+\frac{1}{S_r}\left(\frac{W}{C}\right)\right)+\left(1-G_{s-CRF}\right)\left(1+\frac{1}{B_w}\right)} \tag{5}$$

where:

$G_{s\text{-}CRF}$ = specific gravity of the CRF mixture (which can be taken as equal to that of the WR $G_{s\text{-}WR}$).

$\rho_{s\text{-}CRF}$ = specific density of the CRF mixture (equal to that of the WR, $\rho_{s\text{-}WR}$) in gcm^{-3}, kgm^{-3} or tm^{-3}.

W/C = water-to-cement/binder ratio.

S_r = degree of saturation in decimal form (it should be noted that S_r of CRF can vary between 20 and 70%).

B_w = binder rate (in decimal form).

It should be noted that the porosity of CRF can vary between 11.7 and 34.7% (Annor 1999).

2.2 Sample application: effect of the W/C ratio

Figure 1 presents a graphical representation of the semi-empirical model presented in Equation 1. The predicted UCS is represented as a function of the W/C ratio for different $B_{w\%}$. A clear decrease in the predicted UCS is observed, which means that the increase of water content (*w*) will result in the reduction of the UCS. This non-linear trend confirms not only that the parameter W/C ratio is important and must be optimised

and controlled, but also that the proposed semi-empirical model for the prediction of the uniaxial compressive strength seems efficient.

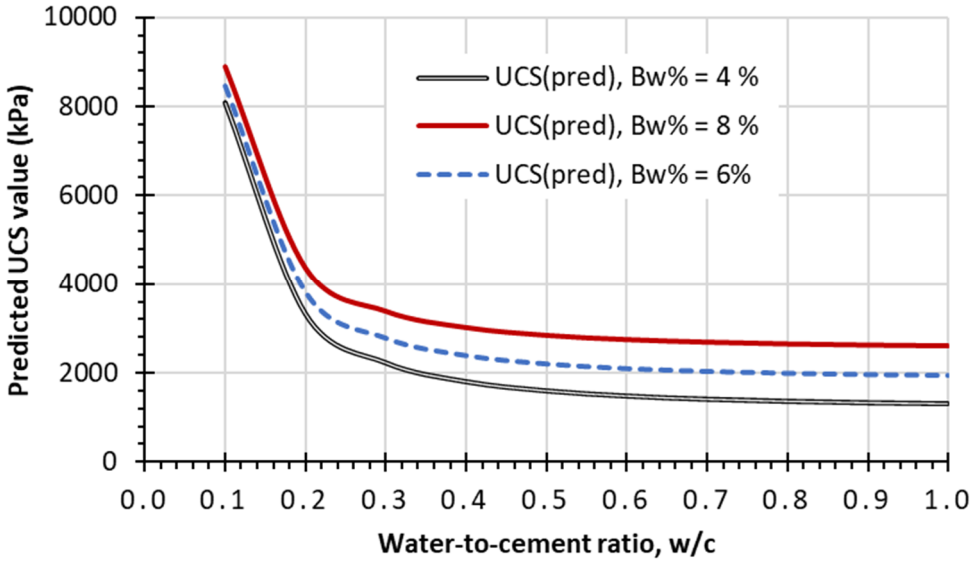

Figure 1 Variation in the predicted UCS as a function of W/C: binder 10GU/90Slag and curing time *t* = 7 days

2.3 Sample application: effect of the curing time

The curing time is a major factor when predicting the uniaxial compressive strength of cemented rockfills. Figure 2 presents sample applications of the predictive model (Equation 1) showing a comparative evolution over the course of the curing time of the predicted UCS for two types of binder (GU-Slag and GU-FA) and for three different binder rates (4, 6 and 8%). A slight non-linear evolution of the predicted UCS as a function of curing time can be clearly observed with the GU-Slag binder, whereas this evolution becomes linear when the GU-FA binder is used. It should be noted that the semi-empirical model makes it possible to predict the UCS of the CRF in fresh conditions, namely at curing time *t* = 0. Considering the quality control of CRF strength, predicting the early age UCS values is advantageous. Indeed, it offers the possibility of estimating whether the CRF mixture will develop enough strength to comply with the required compressive strength during the course of the curing time.

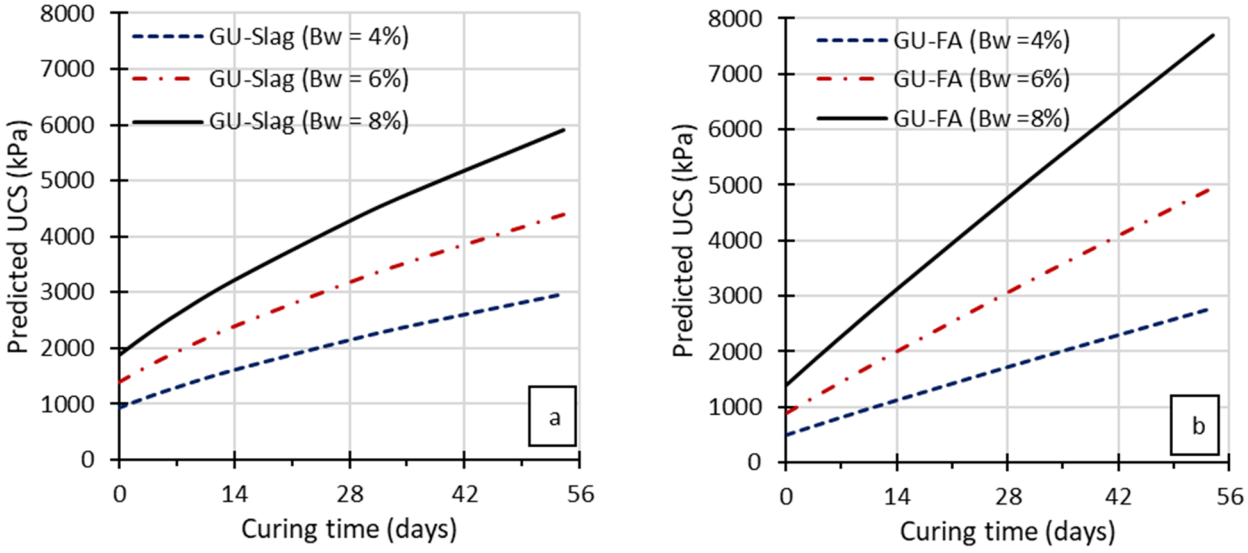

Figure 2 Predicted UCS as function of the curing time (t) for a two water-to-cement ratio and different ratio of two types of binder: (a) 10GU/90Slag and W/C = 1, (b) 50GU/50FA and W/C = 1

3 Methodology

3.1 Waste rock

The WR used in this study were sampled from the Canadian Malartic mine in Quebec, Canada. This WR is characterised by a mean diameter between 0 and 50 mm. After receiving the samples, the WR were first homogenised using a shovel and then stored in plastic barrels until the different laboratory characterisations and tests were conducted. The characterisation tests were to determine the G_s or D_R and the PSD of the WR. It should be noted that it is preferable that the gravimetric water content ($w = M_{water}/M_{solid}$) of the crushed WR does not exceed 5% in order not to increase the W/C ratio, which could lead to a reduction in the uniaxial compressive strength (Yu 1989; Stone 2007; Vennes 2014). In this study, the gravimetric water content of the WR was determined to be w = 2.5%, which is acceptable.

3.1.1 Determination of the G_s of WR

To determine the G_s of the WR, an 11 kg sample was taken. Then coarse particles and fine particles were separated by sieving, as shown in Figure 3.

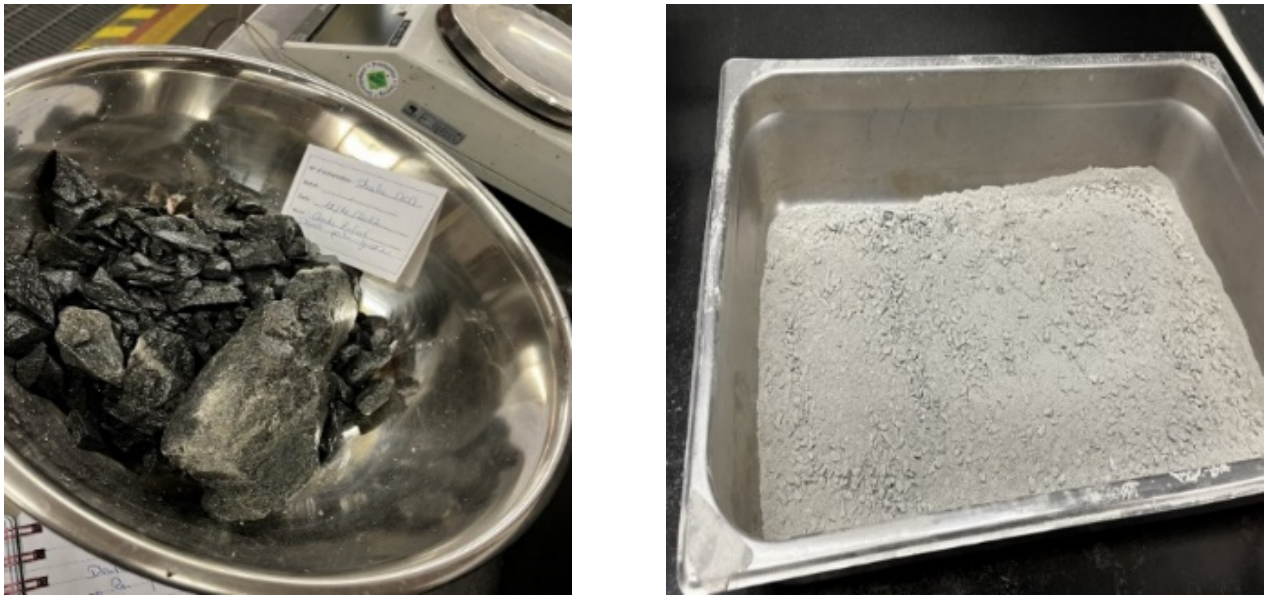

(a) (b)

Figure 3 WR separated in two size fractions: (a) Coarse particles of the sample; (b) Fine particles of the sample

In accordance with ASTM C128 standard (ASTM International 2015), the G_s of the fine particles was determined using a helium pycnometer (AccuPyc 1330 from Micromeritics) and the value of 2.795 was obtained. Using a water basin, the solids specific density (ρ_s) of the coarse particles of WR was determined to be 2,805 kg/m^3. Knowing that the G_s is equal to the ratio of the ρ_s of WR and the density of water at 4°C, which is 1.000 ($G_s = \rho_s/\rho_w$), the average G_s of the WR was determined to be 2.8.

3.1.2 Determination of the PSD

In accordance with ASTM C136 standard test method (ASTM International 2006), the particle size distribution (PSD) was determined by sieving. A large-scale device was used to separate the coarse particles using different meshes (56, 40, 28, 20, 14, 10 and 5 mm) (Figure 4a) and superposed sieve screens was used (openings of 80, 160, 315, 630, 1,250, 2,500 µm) to separate the fine particles (Figure 4b).

(a) (b)

Figure 4 Large-scale device to separate the coarse aggregate (a) and superposed sieves to separate the fine aggregate (b)

Figure 5 presents the PSD curve of the WR received from the Canadian Malartic mine. In the practice of CRF, it is customary to consider particles of size ≤ 10 mm (1 cm) as the fine fraction of the WR. Based on field observations, an optimal CRF mixture should contain at least 25 to 40% fine particles (Vennes 2014). In addition, as shown in Figure 5, the WR contains approximately 39% fine particles.

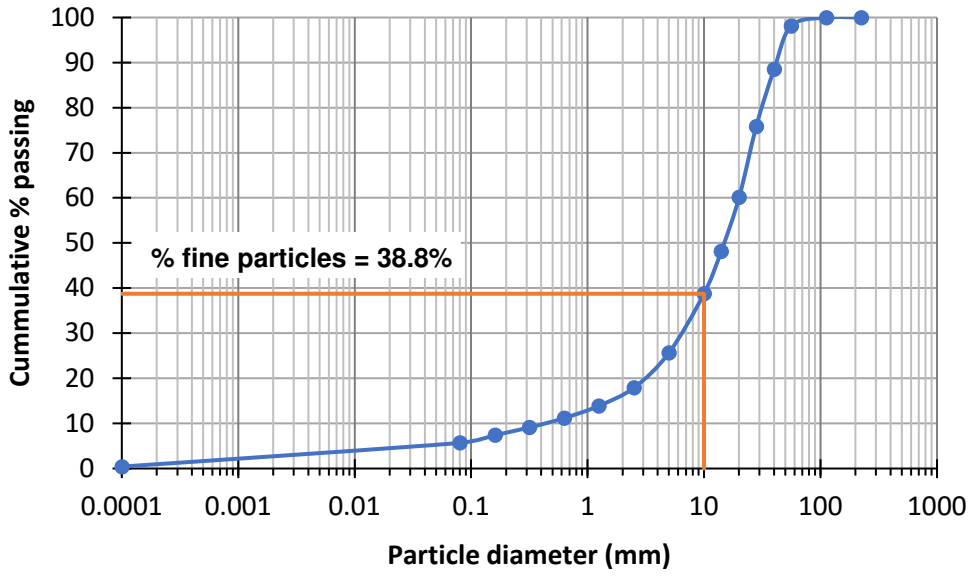

Figure 5 PSD curve of the WR from Canadian Malartic mine

Table 2 highlights all the important particle size parameters of the W that will be used in the CRF specimens' preparation. It can be noted that the values of C_u = 47.48 and C_C = 4.72 are consistent with the range of values that can be found in the literature. Indeed, according to Annor (1999), the C_C values for the rockfill aggregates ranged between 1.44 and 6.54, while C_U values varied between 9.15 and 59.7.

Table 2 Physical characterisation of WR

Parameter	Units	Value
$C_u = D_{60}/D_{10}$	(–)	47.48
$C_c = D_{30}^2/(D_{60} \times D_{10})$	(–)	4.72
$U = (D_{90} - D_{10}) / D_{50}$	(–)	2.82
D_{10}	mm	0.42
D_{20}	mm	3.01
D_{30}	mm	6.27
D_{40}	mm	10.44
D_{50}	mm	14.78
D_{60}	mm	19.89
D_{70}	mm	24.70
D_{80}	mm	31.48
D_{90}	mm	42.08
%fine particles	(–)	38.40

3.2 Mixing water

Mixing water is used to dissolve the binder and lubricate the final CRF mix to facilitate the plastic mould pouring. It is usually tap water or recycled process water instead of sulfated water which could inhibit the CRF hardening process or lead to a strength loss due to internal sulfate attack (Benzaazoua et al. 2002, 2004). Tests conducted at the Kidd Creek mine (Ontario, Canada) have demonstrated that using recycled mine water can reduce the compressive strength of the CRF by 50% compared to CRF prepared with tap or potable water (Gélinas 2021). Therefore, tap water will be used for the CRF mixes preparation.

3.3 Binder

Binder is the most important component in CRF because its type (chemical composition) directly affects the compressive strength development. In mining industry practice, CRF is usually prepared using GU slurry. To reduce costs while improving compressive strength gains, mineral additive such as ground granulated blast furnace slag or types C and F fly ash are very often blended with GU to be used as binding agent in the CRF mix preparation. In this study, two types of binder were considered: 10% GU/90% slag (or 10GU/90Slag) and 50% GU/50% fly ash (FA) type C (or 50GU/50FA).

3.4 CFR mixtures preparation

Two types of binder (10GU/90Slag and 50GU/50FA), two water-to-cement ratio values (W/C = 0.8 and 1), three binder rates $B_{w\%}$ (4, 6 and 8%) were chosen for different CRF mixtures preparation. The CRF specimens were prepared in triplicate and for two curing times *t* (7 and 28 days) for a total of 72 specimens tested. Table 3 summarises all the CRF mix recipes formulated.

Table 3 CRF mix recipes formulation

Types of binder	Binder rate $B_{w\%}$	Water-to-cement ratio	Curing time *t* (days)	Number of specimens
10GU/90Slag or 50GU/50FA	4	0.8	7, 28	2x2x3 = 12
	6	0.8	7, 28	12
	8	0.8	7, 28	12
	4	1.0	7, 28	12
	6	1.0	7, 28	12
	8	1.0	7, 28	12

To mix the CRF ingredients altogether, a drum mixer was used (Figure 6a) to prepare a batch of CRF (Figure 6b) that was quartered (Figure 6c) before pouring into plastic moulds with 15.24 cm diameters and 30.48 cm heights. The three layers of equal thickness are then pounded by 25 blows of a steel tamping rod (Figure 6d). The prepared 72 CRF moulds were then stored in a humid chamber under controlled conditions (temperature of 25 ± 2°C and relative humidity of RH ≥ 90%).

(a) (b) (c) (d)

Figure 6 CRF preparation: (a) Drum mixer; (b) CRF mixing batch; (c) Quartering of the mixing batch; (d) Three filled plastic moulds

3.5 Uniaxial compression tests

After each curing time the moulds are removed from the humid chamber and the CRF specimens are extracted and capped. Then the specimens are subjected to uniaxial compression testing in accordance with ASTM C39/C39 M (ASTM International 2021) using a stiff mechanical press with a loading capacity of 100 kN and run at a constant displacement velocity of 1 mm per minute. The data acquisition system recorded the axial strain and the normal stress applied to the specimens during the test until its failure, which represents the stress-strain curve from which the peak value corresponds to the UCS. It should be noted that each UCS value after each curing time is the average from three values (triplicate).

4 Results and discussion

4.1 Unconfined compressive strength

Tables 4 and 5 show the results of uniaxial compression tests on specimens prepared from the different CRF mix recipes. For the GU-Slag binder, the experimental values were 4,508 kPa (max.), 1,329 kPa (min.) and 2,777 kPa (average). For the GU-FA type binder, the experimental values were 5,093 kPa (max.), 1,002 kPa (min.) and 2,713 kPa (average).

Table 4 Values of experimental and predicted values of UCS for different recipes (binder type 10GU/90Slag)

Curing time (days)	W/C (–)	$B_{w\%}$ (%)	Experimental UCS (kPa)	Predicted UCS (kPa)	$UCS_{pred} - UCS_{exp}$ (kPa)
7	0.8	8	2,788	2,613	-175
7	1	8	3,211	2,595	-616
7	0.8	6	1,329	1,977	648
7	1	6	1,896	1,928	32
28	0.8	8	4,208	4,350	142
28	1	8	4,508	4,276	-232
28	1	4	1,500	2,147	647

Table 5 Values of experimental and predicted values of UCS for different recipes (binder type 50GU/50FA)

Curing time (days)	W/C (–)	$B_{w\%}$ (%)	Experimental UCS (kPa)	Predicted UCS (kPa)	$UCS_{pred} - UCS_{exp}$ (kPa)
7	1	4	1,002	821	-181
7	0.8	6	1,670	1,522	-148
7	1	6	1,949	1,466	-483
7	1	8	2,238	2,275	37
7	0.8	8	4,000	2,334	-1,666
28	1	4	1,756	1,719	-37
28	1	6	3,157	3,069	-88
28	1	8	3,549	4,763	1,214
28	0.8	8	5,093	4,886	-207

4.2 Performance metrics of the UCS prediction

The performance metrics evaluated in this paper are the linear regression correlation coefficient (R), the root mean squared error (RMSE), and the normalised RMSE, which are given by the following equations:

$$\mathrm{R} = \frac{\sum_{j=1}^{N}\left(y_j - \overline{y}_j\right)\left(\hat{y}_j - \overline{\hat{y}}_j\right)}{\sqrt{\sum_{j=1}^{N}\left(y_j - \overline{y}_j\right)^2}\sqrt{\sum_{j=1}^{N}\left(\hat{y}_j - \overline{\hat{y}}_j\right)^2}} \tag{6}$$

$$\mathrm{RMSE} = \sqrt{\frac{1}{N}\sum_{j=1}^{N}\left(y_j - \hat{y}_j\right)^2} \tag{7}$$

$$\text{Normalized RMSE} = \sqrt{\frac{1}{N}\sum_{j=1}^{N}\left(y_j - \hat{y}_j\right)^2} \Big/ \left[y_{j-\max} - y_{j-\min}\right] \tag{8}$$

where:

y_j and $\hat{y}_j$ = the experimental values and the predicted values.

$\bar{y}_j$ and $\overline{\hat{y}}_j$ = the average of the experimental and predicted values.

$y_{j\text{-min}}$ and $y_{j\text{-max}}$ = the minimum and maximum experimental values and the predicted values.

N = the total number of data points of the considered sample.

The normalised RMSE produces a value between 0 and 1, where values closer to 0 represent better fitting/prediction models.

Figure 7 shows the affine linear regression lines (dashed) between the predicted and experimental UCS for the GU-Slag binder (Figure 7a) and the GU-FA binder (Figure 7b). It can be noted that the correlation coefficient is R = 0.99 for the predictions with the GU-Slag binder and R = 0.97 for the predictions with the GU-FA binder. Also shown in these figures are the 1:1 slope lines.

The coefficient of correlation R indicates how strong the relationship between the experimental and the predicted uniaxial compressive strength. The high value of R (close to 1) means an excellent linear relationship between experimental values and predicted values obtained using the semi-empirical model (Eq. 1). Consequently, the semi-empirical predictive model can be considered efficient and accurate.

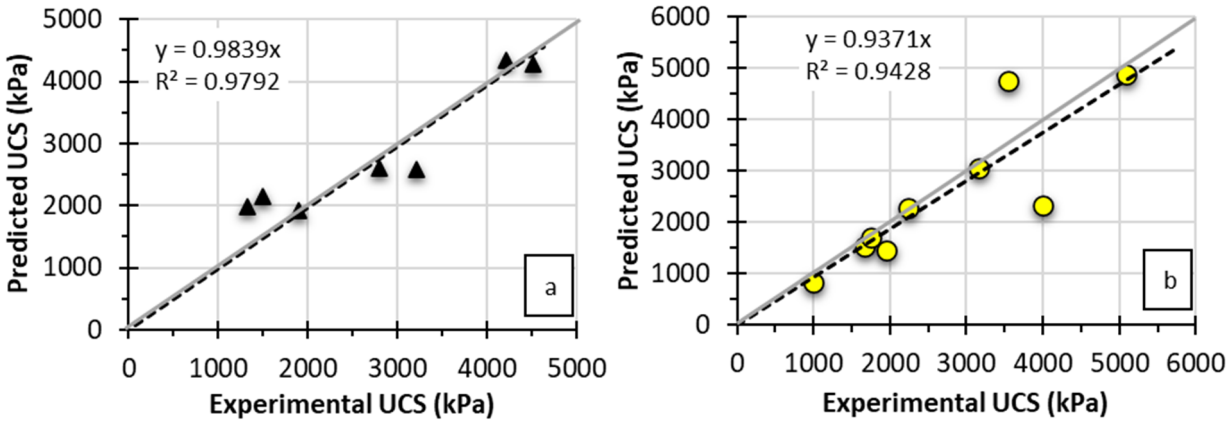

Figure 7 Linear regression curves for (a) 10GU/90Slag binder; (b) 50GU/50FA binder

Table 6 contains the experimental minimum and maximum UCS values as well as the RMSE and normalised RMSE. The closer the RMSE is to 0, the better the model prediction is. With normalised RMSE values of 0.14 and 0.17 it can be concluded that the predictions made using the semi-empirical model (Eq. 1) are very reasonable and acceptable.

Table 6 RMSE and normalised RMSE values of predicted UCS

Binder	UCS_{min} (kPa)	UCS_{max} (kPa)	RMSE (kPa)	Norm. RMSE (–)	R (–)
10GU/90Slag	1,329	4,508	434.8	0.14	0.99
50GU/50FA	2,777	1,329	714.2	0.17	0.97

5 Conclusion

This study aims to validate experimentally a new semi-empirical model recently developed for predicting the UCS of CRF. From this study, the following conclusions can be drawn:

- The new semi-empirical model seems a versatile solution for better predicting the UCS while taking into consideration several physical and mix design parameters such as the W/C ratio, the types of binder (slag-based or fly ash-based), the $B_{w\%}$, the WR particles gradation (D_{50} and d_{min}), the WR relative density (G_s) and the CRF curing time.
- The semi-empirical model can estimate the UCS in an efficient manner when varying the curing time, which is a main parameter in the process of the required strength development.
- Comparing experimental and predicted uniaxial compressive strength has shown a correlation coefficient (R) that is close to 1 and an RMSE that is relatively low (<0.2). This means that the semi-empirical model is reliable and accurate.
- The semi-empirical model will provide the opportunity of developing an efficient CRF production QC procedure.

Acknowledgement

The authors would like to thank their university, Université du Québec en Abitibi-Témiscamingue, and the Government of Canada for their financial support through the Research and Creation Grants – Support for the realisation of short projects (#FIRC/FUQAT 2021-2022), and the NSERC Discovery Grant (#RGPIN-2019-04946) respectively. The authors would also like to acknowledge AEM Ltd for its partnership and financial support through the Research Institute of Mines and Environment.

References

Annor, AB 1999, *A Study of the Characteristics and Behaviour of Composite Backfill Material*, PhD thesis, McGill University, 396 p.

Arioglu, E 1984, 'Design aspects of cemented aggregate fill mixes for tungsten stoping operations', *Mining Science and Technology*, pp. 209–214.

ASTM 2006, *Standard Test Method for Sieve Analysis of Fine and Coarse Aggregates (C136)*, ASTM International, West Conshohocken, pp. 3–7, http://dx.doi.org/10.1520/C0136-06

ASTM 2015, *Standard Test Method for Relative Density (Specific Gravity) and Absorption of Fine Aggregate (C128-15)*, ASTM International, West Conshohocken.

ASTM 2021, *Standard Test Method for Compressive Strength of Cylindrical Concrete Specimens (*C39/C39 M), ASTM International, West Conshohocken.

Belem, T & Benzaazoua, M 2008, 'Design and application of underground mine paste backfill technology, *Geotechnical and Geological Engineering*, vol. 26, no. 2, pp. 147–174.

Belem, T 2020, 'Semi-empirical models for predicting the unconfined compressive strength of virtual uncemented rockfill (RF) and cemented rockfill (CRF), internal report, Research Institute on Mines and Environment, Montreal, 19 p.

Benzaazoua, M, Belem T & Bussière, B 2002, 'Chemical aspect of sulphurous paste backfills mixtures, *Cement and Concrete Research*, vol. 32, no. 7, pp. 1133–1144.

Benzaazoua, M, Fall, M & Belem, T 2004, 'A contribution to understanding the hardening process of cemented pastefill, *Minerals Engineering*, vol. 17, no. 2, pp. 141–152.

Farsangi, PN 1996, *Improving Rockfill Design in Open Stoping*, PhD thesis, McGill University, Montreal.

Farsangi, PN, Hayward, AG & Hassani, FP 1996, 'Consolidated rockfill optimization at Kidd Creek Mines, *CIM Bulletin*, vol. 89, no. 1001, pp. 129–134.

Gonano, LP, Kirkby, RW & Dight, PM 1978, *Triaxial Testing of Cemented Rockfill*, technical report 72, Commonwealth Scientific and Industrial Research Organisation, Australia.

Gélinas, LP 2021, *Current Knowledges on Arctic Cemented Rockfill (CRF) Cured in Permafrost Conditions*, internal AEM document #6128-000-100-TCR-001, technical report.

Hane, I, Belem, T & Benzaazoua, M 2018, *Cemented Rock Fill (CRF) Plant Laboratory Test Methods for Kirkland Lake Gold (KL)*, final report PU-2017-11-1172, 23 p.

Hane, I, Belem, T, Benzaazoua, M & Maqsoud, A 2017a, 'Laboratory characterization of cemented tailings paste containing crushed waste rocks for improved compressive strength development,' *Geotechnical and Geological Engineering*, vol. 35, no. 2, pp. 645–662, https://doi.org/10.1007/s10706-016-0131-6

Hane, I, Belem, T, Benzaazoua, M & Maqsoud, M 2017b, 'Laboratory investigation into the compressive strength of cemented paste tailings aggregate fills', in M Hudyma & Y Potvin (eds), *UMT 2017: Proceedings of the First International Conference on Underground Mining Technology*, Australian Centre for Geomechanics, Perth, pp. 363–373, https://doi.org/10.36487/ACG_rep/1710_28_Hane

Hedley, DGF 1995, *Final Report on the Stiff Backfill Project for M.R.D.*, Mining Research Directorate, Canadian Rockburst Research Program, Sudbury.

Lamos, AW & Clark, IH 1993, 'The influence of material composition and sample geometry on the strength of cemented backfill', *Innovations in Mining with Backfill: Proceedings of the Fourth International Symposium on Mining Backfill*, A.A. Balkema, Rotterdam, pp. 89–94.

Mitchell, R, & Wong, B 1982, 'Behaviour of cemented tailings sands', *Canadian Geotechnical Journal*, vol. 19, no. 3, pp. 289–295.

Stone, DMR 1993, 'The optimization of mix designs for cemented rockfill', *Minefill*, vol. 93, pp. 249–253.

Stone, DMR 2007, 'Factors that affect cemented rockfill quality in Nevada Mines', *CIM Bulletin*, vol. 100, no. 1103, pp. 1–6.

Villaescusa, E 2003, 'Global extraction sequences in sublevel stoping', *Proceedings of the 12th International Symposium on Mine Planning and Equipment Selection,* vol. 1, pp. 9–17.

Vennes, I 2014, *Determination of Cemented Rockfill Strength with Large Scale UCS Tests Under In-situ Conditions*, master's thesis, McGill University, Montreal.

Yu, T 1989, 'Some factors relating to the stability of consolidated rockfill at Kidd Creek', *Innovations in Mining Backfill Technology*, CRC Press, Boca Raton, pp. 279–286.